Advances in Accelerator Physics at NSLS-II

Victor Smaluk

NSLS-II

Outline

- Analysis of nonlinear dynamics by square matrix method.
- Linear lattice correction techniques based on turn-by-turn BPM data:
  - ✓ Independent Component Analysis (ICA);
  - ✓ Driving-Terms-Based Linear Optics Calibration.
- AC LOCO – a fast and precise technique for magnet lattice correction.
- AC orbit bump method of local impedance measurement.
- Real-time redistribution of the fast correctors' strengths to the paired slow correctors.
- Lossless crossing of a half-integer resonance.
- New unique capability of NSLS-II BPMs: gated turn-by-turn BPM data.
  - ✓ Single-shot measurement of the tune shift with amplitude;
  - ✓ High-resolution measurement of current-dependent tune shifts.
- Low-frequency quadrupole impedance of undulators and wigglers.
- Microwave instability studies.
- Fast-ion instability at NSLS-II.
- Beam dynamics with 3rd Harmonic Cavity.
- Self-consistent Parallel Tracking Code.
- High-brightness lattice upgrade options for NSLS-II.

Analysis of nonlinear dynamics by Square Matrix Method.

L.-H. Yu, "Analysis of nonlinear dynamics by square matrix method",
Phys. Rev. Accel. Beams 20, 034001 (2017)

- Nonlinear dynamics of a system with periodic structure is analyzed using a square matrix. This is a novel method to optimize the nonlinear dynamic system. The method is illustrated by examples of comparison between theory and numerical simulation.
  - Square matrix $Z = MZ_0$
  - **One step** to high order without iteration $UM = e^{i\mu I+\tau}U$
  - Action-angle approximation $W \equiv UZ = \begin{bmatrix} w_0 \\ w_1 \\ \cdots \\ w_m - 1 \end{bmatrix}$ $\quad W = e^{i\mu I+\tau}W_0 \cong e^{i(\mu+\phi)}W_0.$
  - **Amplitude-dependent tune** ϕ

    Action $|w_0|$ **s nearly a constant:** $|\frac{\Delta W}{W}| \approx 0$
  - **Frequency fluctuation** $\Delta \equiv \frac{w_2}{w_0} - (\frac{w_1}{w_0})^2 \approx 0$

    Amplitude fluctuation $|\frac{\Delta W}{W}|$

Phase space transformation

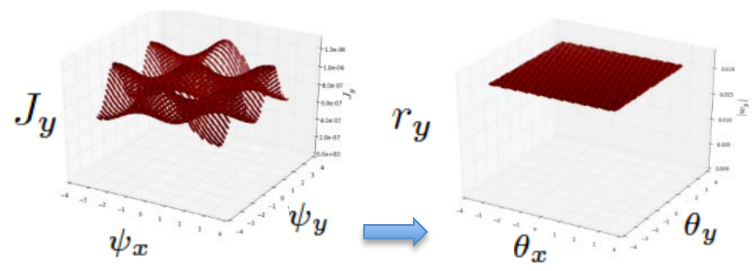

Phase space manipulation by Square Matrix Method

L.-H. Yu, Y. Li

- minimization of $|\Delta w/w|$ 5 particles with initial y increases proportional to initial x

Conventional optimization

1000 turns

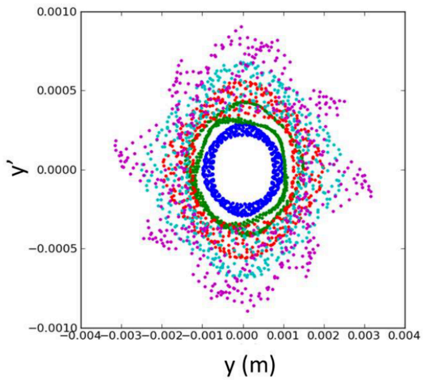

15000 turns

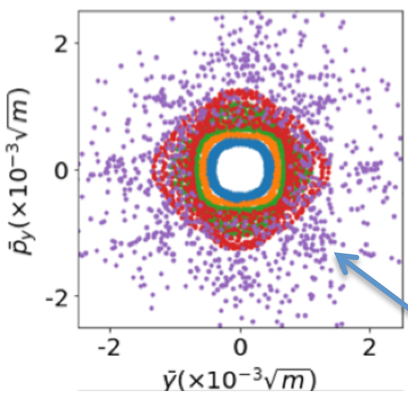

Square matrix optimization

1000 turns

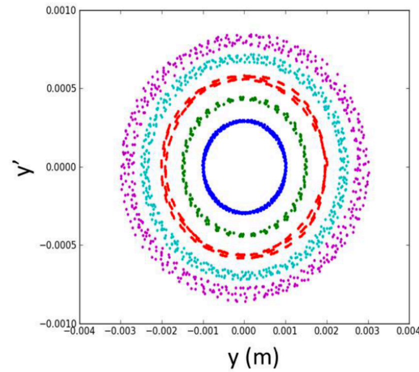

15000 turns

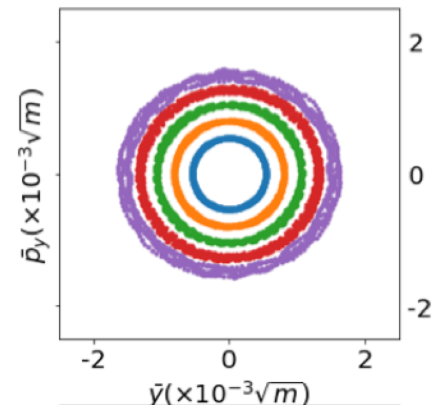

Particles diffused into much larger amplitudes.

Particles are lost in top left corner

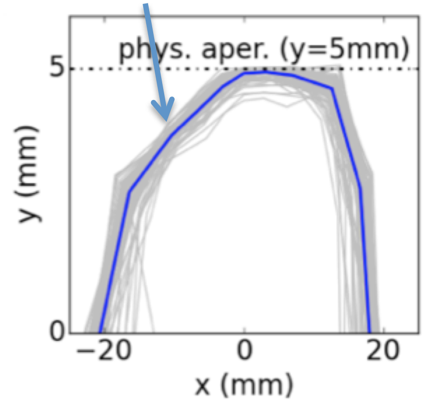

Spectrum is much more wide and complicated.

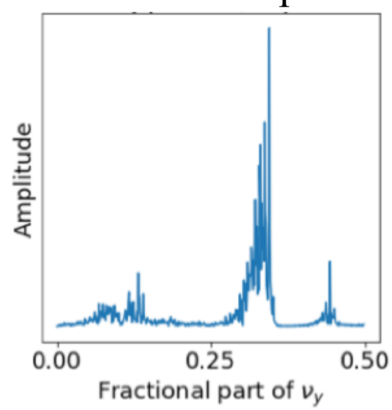

DA is more symmetric

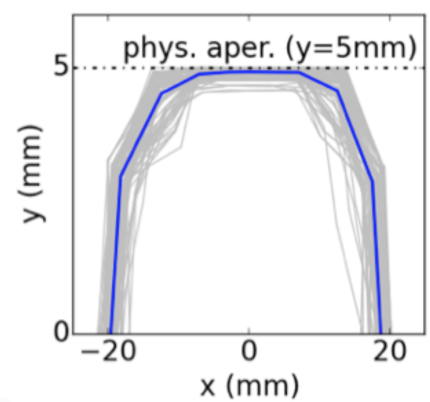

Spectrum is narrow.

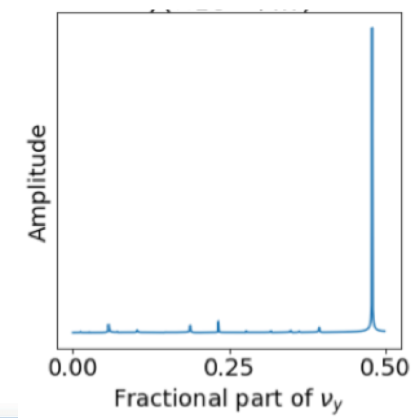

ICA turn-by-turn based lattice tool

X. Yang, X. Huang, "A method for simultaneous linear optics and coupling correction for storage rings with turn-by-turn beam position monitor data", NIM A 828, p97-104 (2016).

- The independent component analysis (ICA) method for simultaneous linear optics and coupling correction turn-by-turn BPM data has been tested at NSLS-II.
- The ICA method is first applied to extract the amplitudes and phases of the projection of the normal modes on the horizontal and vertical BPM turn-by-turn data, which are then compared to their model-generated counterparts in fitting.
- The fitting scheme is similar to the LOCO algorithm.
- The method provides similar precision of BPM calibration and residual errors of linear lattice compared to the standard LOCO technique.
- Software is ready to release.
- Plan to improve the speed of calculation using parallel computing.

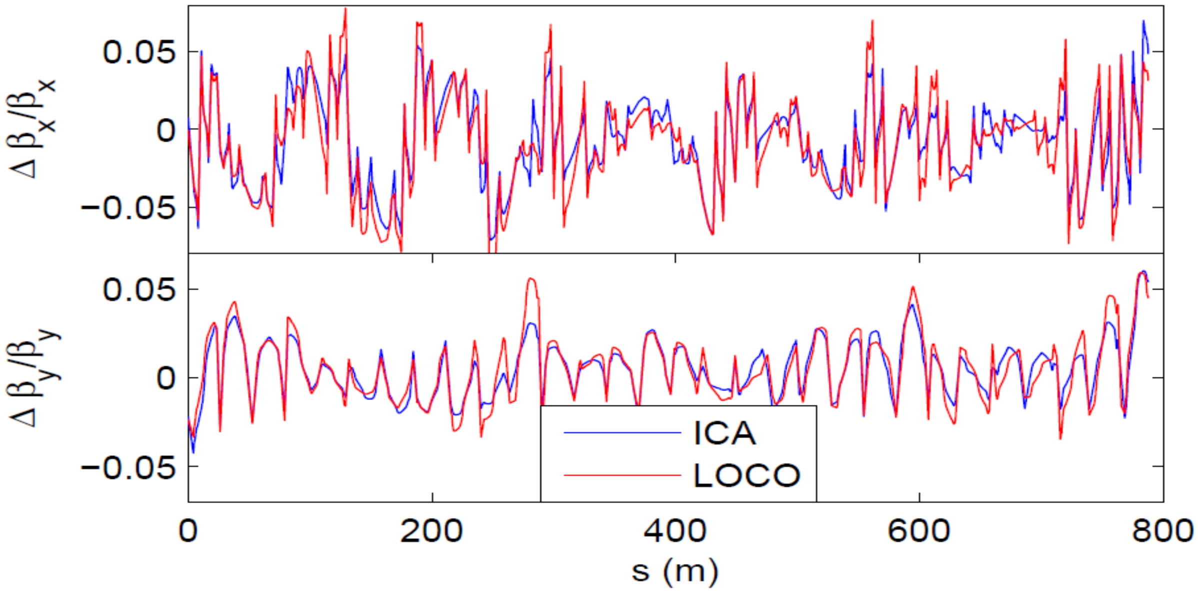

Driving-terms-based linear optics calibration

Y. Hidaka, B. Podobedov, J. Bengtsson, "Linear optics characterization and correction method using turn-by-turn BPM data based on resonance driving terms with simultaneous BPM calibration capability", NAPAC'16, Chicago, 2016 (TUPOB52).

- The DTBLOC (Driving-Terms-Based Linear Optics Calibration) algorithm implemented in a Python code.
- Input (Observables): 4 frequency components extracted from turn-by-turn (TbT) data & dispersion functions.
- Output (fitting parameters): normal & skew quad. errors, BPM errors (hor./ver. gain, roll & deformation).
- Iterative least-square fitting via SVD with analytical Jacobian based on resonance driving terms (RDTs).
- Very fast! Only needs ~5 minutes for data acquisition, processing and fitting (vs. ~1 hour to measure full ORM for LOCO) at NSLS-II.
- Corrected to ~1% beta-beating, dispersion errors of ~1 mm, emittance coupling ratio on the order of 0.1%.
- Also works as a validation tool for estimated magnetic and BPM error values.

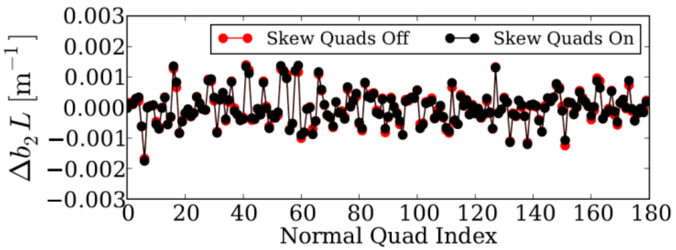

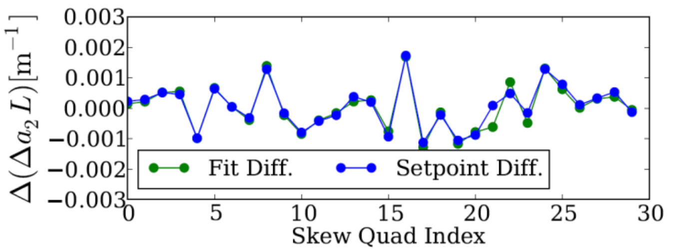

Example: For bare lattice, brought ε_y from 100 pm (all skew quads off) down to 2-3 pm, while reducing lifetime from 190 to 26 hr for 2 mA/100 bunches, with 2 iterations taking 10 min.

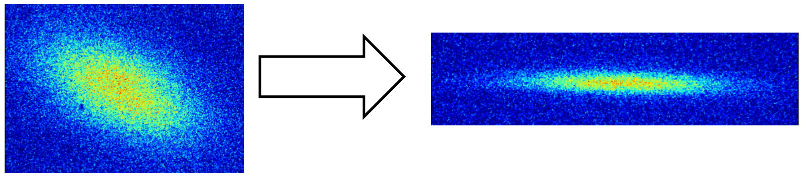

Application: Table generation for global coupling feedforward system for C17-1 IVU: after 1 iteration (12 gap values for 25 min. meas. & 25 min. proc.), closed-vs-open-gap difference of $(\Delta\sigma_y, \Delta\tau)$ = (+25%, +38%) reduced to (-1%, +11%)

AC LOCO

X. Yang, V. Smaluk, L.H. Yu, Y. Tian, K. Ha,
"Fast and precise technique for magnet lattice correction via sine-wave excitation of fast correctors", Accepted for publication in Phys. Rev. Accel. Beams (2017).

Measurement

- Sine-wave (AC) beam excitation via fast correctors.
- Possibility of simultaneous excitation of many correctors with different frequencies.
- Recording BPM fast acquisition (10 kHz) data (all BPMs – 1 response vector).
- Synchronous detection of the beam oscillation amplitude.

Correction – standard LOCO technique

- Fitting the measured orbit response matrix to the model.
- Quadrupole strengths.
- Gains and rolls of BPMs and correctors.

Experimental results

- A factor of 2 to 5 reduction in the residual beta-beating and dispersion errors.
- Multi-frequency excitation of 30 fast correctors. Measurement time: < 2 mins for 10s BPM data.

Noise-induced BPM errors at 20 Hz

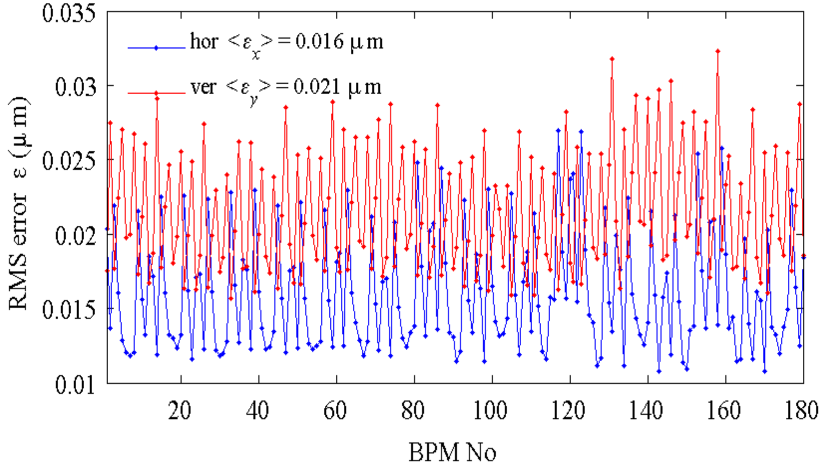

Multi-frequency excitation

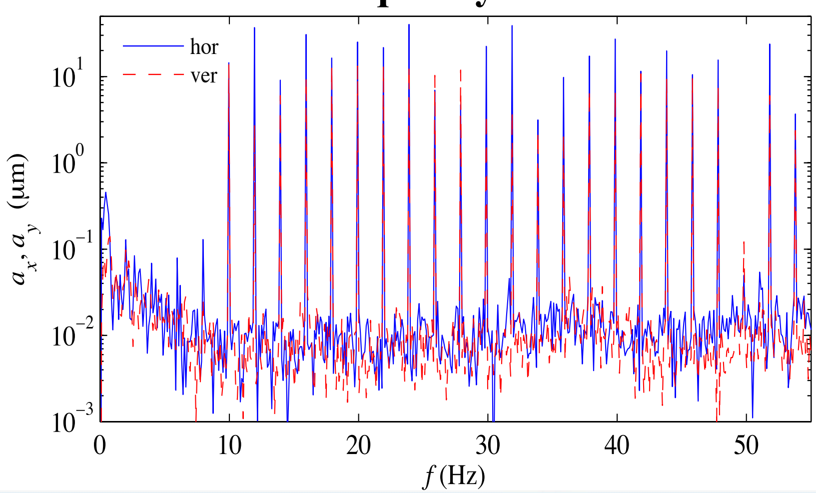

Experimental crosscheck of lattice correction algorithms

V. Smaluk, X. Yang, W. Guo, Y. Hidaka, G. Wang, Y. Li, L. Yang, "Experimental crosscheck of algorithms for magnet lattice correction", IPAC'16, Busan, 2016 (THPMR008).

- Performance, capabilities and limitations of several algorithms for linear magnet optics correction have been studied experimentally at NSLS-II.
- 4 algorithms based on turn-by-turn beam position analysis:
  - ✓ weighted correction of betatron phase and amplitude;
  - ✓ independent component analysis;
  - ✓ model-independent analysis;
  - ✓ and driving-terms-based linear optics characterization.
- LOCO algorithm based on closed orbit measurement has been used as a reference.

Algorithm	$\Delta\beta_x/\beta_x$ %	$\Delta\beta_y/\beta_y$ %	$\Delta\psi_x$ °	$\Delta\psi_y$ °	$\Delta\eta_x$ mm	η_y mm
no corr.	8	10	4.5	3.5	18	8
LOCO	2.1	1.4	0.5	0.2	2.6	4.4
phase only[1]	2.3	1.8	0.6	0.5	39	9.9
phase&amp.[1]	2.8	1.7	0.7	0.9	11	7.8
ICA	2.6	1.6	0.5	0.4	5.0	2.3
MIA	2.8	1.7	0.7	1.0	5.4	6.8
DTBLOC	3.0	1.9	0.4	0.8	2.3	4.5

[1] no dispersion corrected

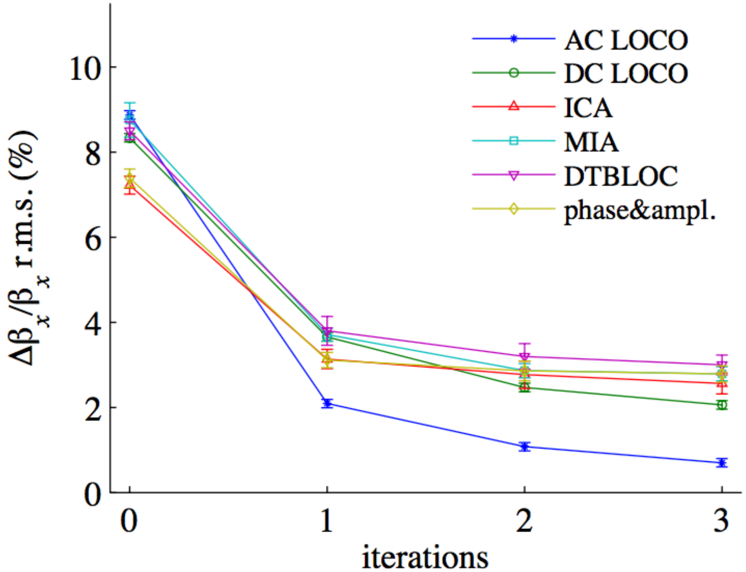

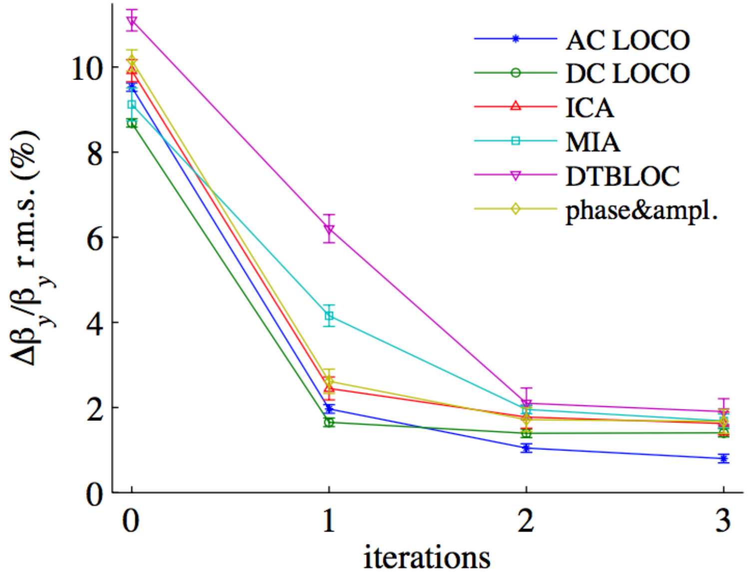

AC orbit bump method of local impedance measurement

V.Smaluk, X.Yang, A.Blednykh, Y.Tian, K.Ha

current-dependent orbit distortion
$$\Delta y(s) = \frac{\Delta q_b}{E/e} k_y \underbrace{y_0}_{\text{bump}} \frac{\sqrt{\beta(s_0)\beta(s)}}{2\sin \pi\nu_\beta} \cos\left(\left|\mu(s)-\mu(s_0)\right| - \pi\nu_\beta\right)$$

AC orbit bump: using 4 fast correctors, in-phase 20 Hz sine-wave excitation

- orbit from 10s FA BPM data (synchronous detection);
- no hysteresis effect, no orbit drift effect.

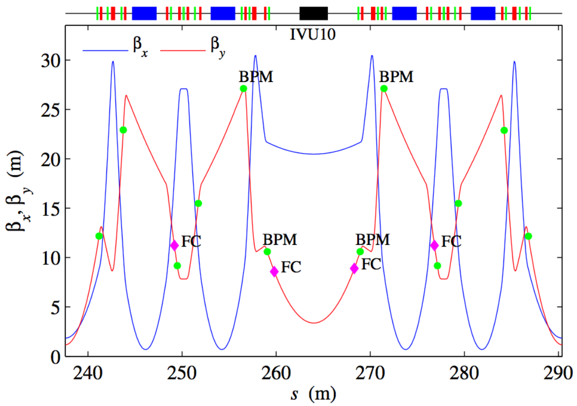

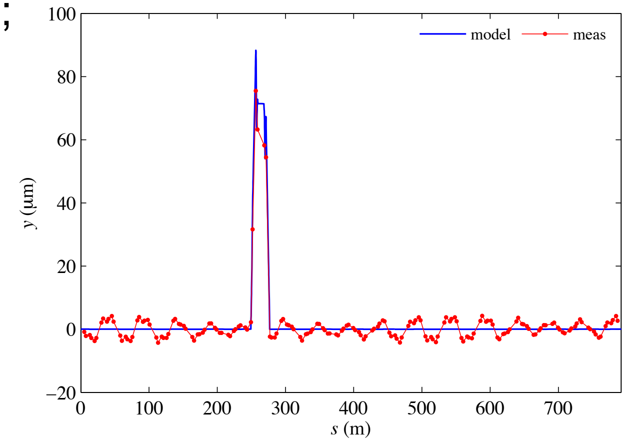

IVU10 gap 6 mm

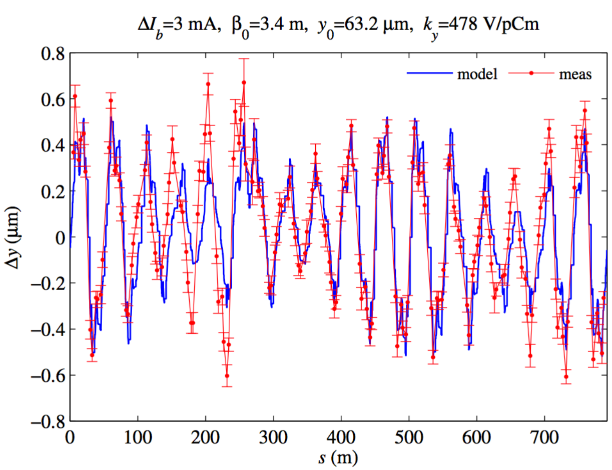

IVU10 gap 25 mm

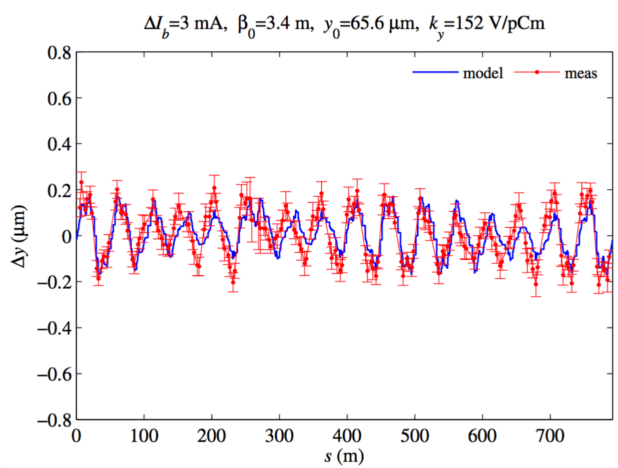

Real-time redistribution of the fast correctors' strengths to the paired slow correctors

X. Yang, Y. Tian, L.-H. Yu, V. Smaluk, "Experimental demonstration of the current shifting between fast and slow correctors in NSLS-II SR when the FOFB on", NSLS-II Technical Note 242 (2017).

- The maximal kick angle of a fast corrector is 0.015 mrad (limited by PS maximal current of 1.2 A).
- Possible reasons of moving fast correctors to saturation: long-term drift, local bumps, changing ID gaps, orbit correction.
- We choose 90 slows correctors, which are paired with 90 fast correctors, to perform the shift. Then there is always a unique solution, which guarantees the convergence.

The procedure, which is applicable to horizontal (X) and vertical (Y) planes separately, is the following:

1. Varying one of 90 slow correctors paired with the fast correctors in bipolar mode ±0.5 A, find the orbit difference ΔX.
2. Correction of the orbit difference ΔX using all 90 fast correctors and the model orbit response matrix. The resulting vector of the fast corrector currents is one column of the slow-to-fast matrix $\mathbf{M}_{s\to f}$.
3. Repeating steps 1 and 2 for all those 90 slow correctors to obtain the full 90×90 slow-to-fast matrix $\mathbf{M}_{s\to f}$.
4. Inverting the square matrix $\mathbf{M}_{s\to f}$ to obtain the fast-to-slow matrix $\mathbf{M}^{-1}_{s\to f}$.

Sum I of all horizontal fast correctors (blue) and sum ΔI of all paired slow correctors (red).

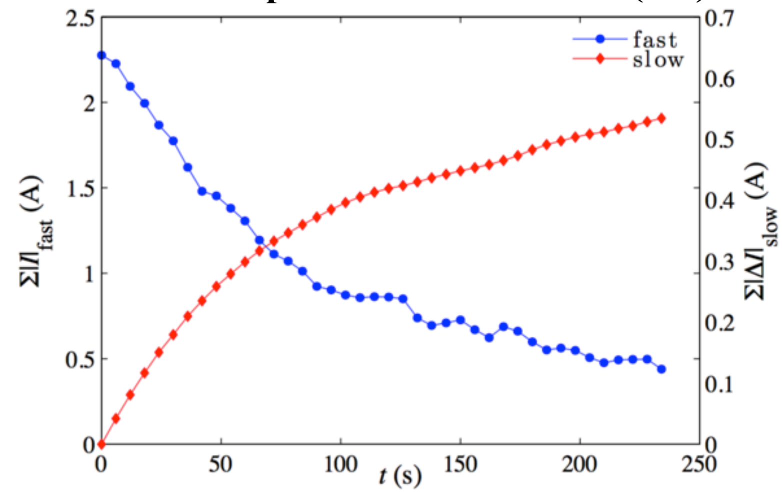

Thus the vector of additional currents $\Delta\mathbf{I}_s$ of these 90 slow correctors required for compensation of the fast corrector currents $\mathbf{I}_f$ is: $\Delta\mathbf{I}_s = \mathbf{M}^{-1}_{s\to f}\mathbf{I}_f$

Lossless crossing of a half-integer resonance

G-M. Wang, T. Shaftan, J. Rose, V. Smaluk, Y. Li, B. Holub, "Experiments of lossless crossing-resonance with tune modulation by synchrotron oscillations", NAPAC'16, Chicago, 2016 (WEPOB65).

- Modern high-performance circular accelerators require sophisticated corrections of nonlinear beam dynamics. The beam betatron tune footprint may cross many resonances, which may cause particle loss and reduce dynamic aperture.
- The half-integer resonance poses concerns in many accelerators, such as modern synchrotron light sources, heavy ion medical accelerators and non-scaling FFAG accelerators.
- Our results convincingly demonstrate that particles can cross a half-integer resonance without being lost if the passage is reasonable fast and the resonance stopband is sufficiently narrow.

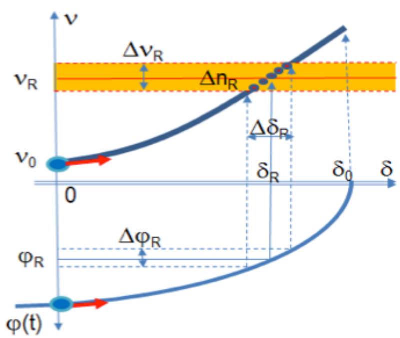

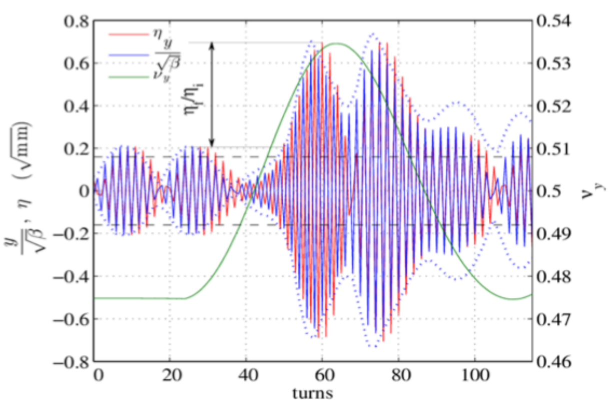

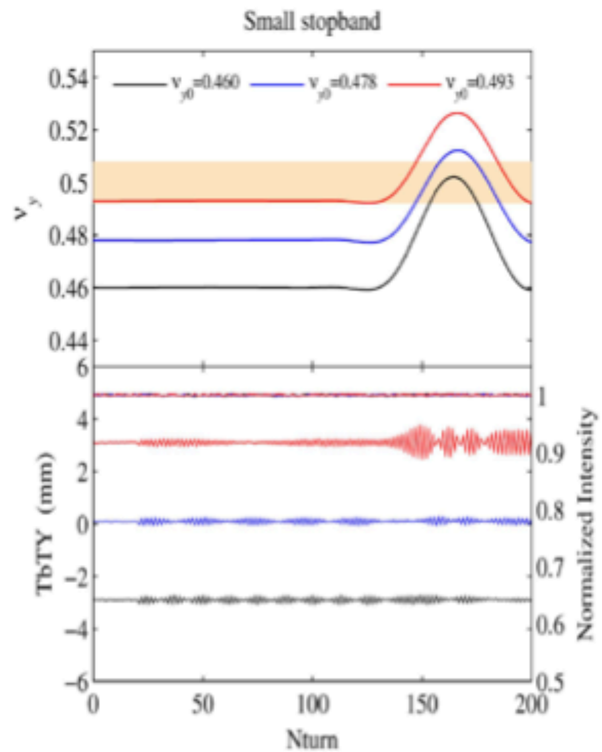

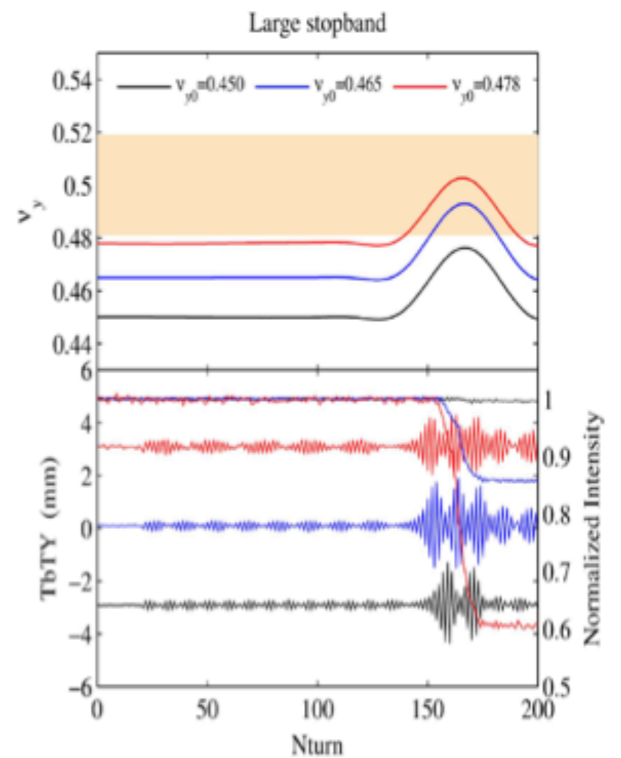

Gated turn-by-turn BPM data

B. Podobedov, W.X. Cheng, K. Ha, Y. Hidaka, J. Mead, O. Singh, K. Vetter. "Single micron single-bunch turn-by-turn BPM resolution achieved at NSLS-II". IPAC'16, Busan, 2016 (WEOBB01).

- Single-bunch resolution of NSLS-II BPMs was improved by an order of magnitude to about one micron turn-by-turn at 1 nC per bunch by special processing of ADC signals.
- The new capability of resolving turn-by-turn signals from up to 8 bunches stored in the ring is useful for sensitive measurements of collective effects or single particle dynamics.
- Having this capability on all NSLS-II RF BPMs is valuable for sensitive measurements of collective effects and non-linear beam dynamics. It allows us to simultaneously measure bunches with different charges (or kick amplitudes) thus eliminating harmful effects of machine drifts.

3 turns of raw ADC data; 0.5 mA single bunch

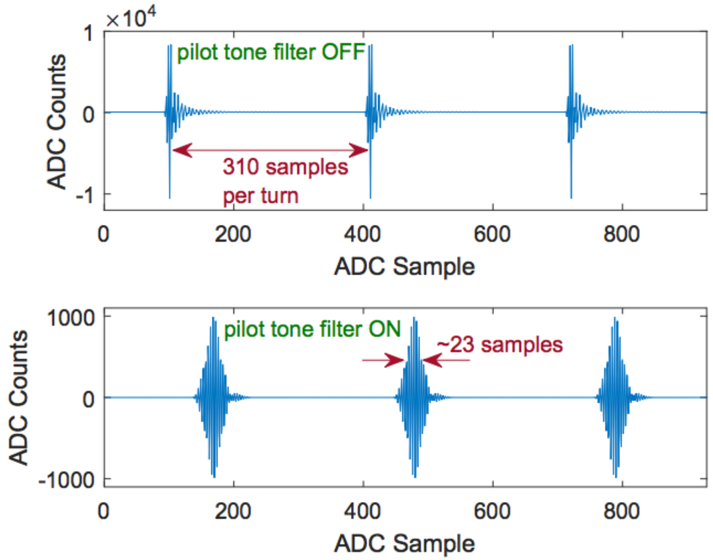

Resolution vs. ADC signal window length

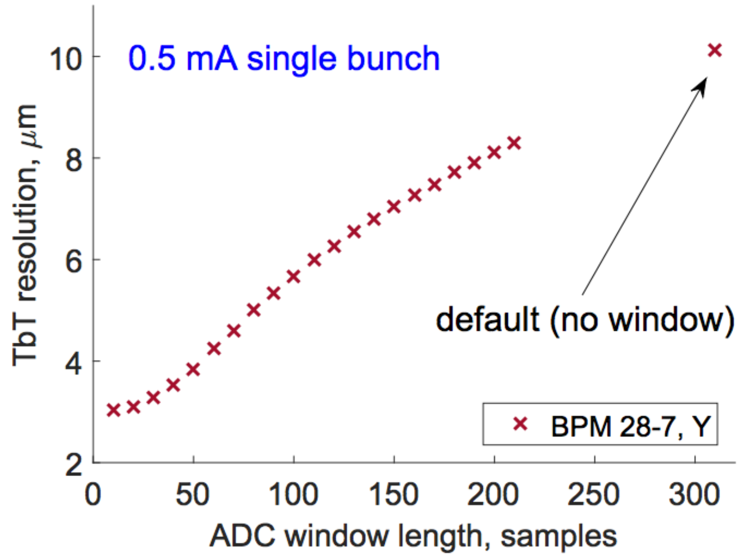

Single-shot measurement of the tune shift with amplitude

Y. Hidaka, W. Cheng, B. Podobedov, NAPAC 2016.

- Accuracy of conventional amplitude-dependent tune shift measurement is affected by short-term tune jitter and long-term machine drift.
- Place trains of bunches in a ring with or without gaps to sample different amplitudes with a single pulse of a kicker.
- Now we need to obtain TbT data for each train kicked with different amplitude.
  - ✓ Data Type #1: New unique NSLS-II BPM capability: Gated turn-by-turn (TbT) BPM data that resolve groups of bunches within a turn.
  - ✓ Data Type #2: Use bunch-by-bunch (BxB) data from BxB feedback system.

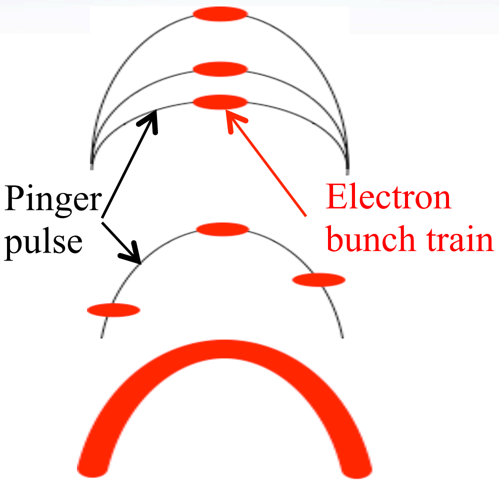

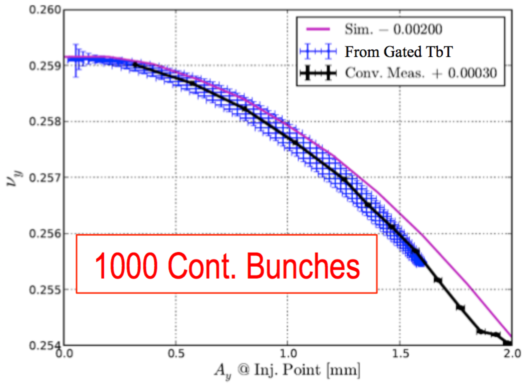

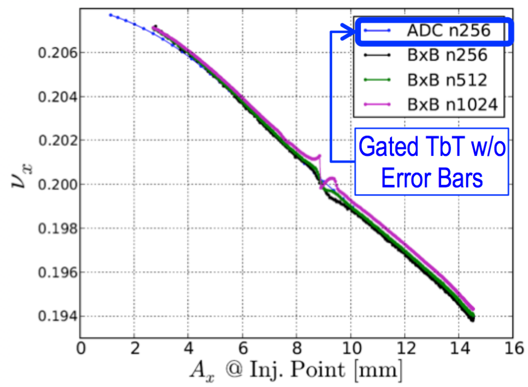

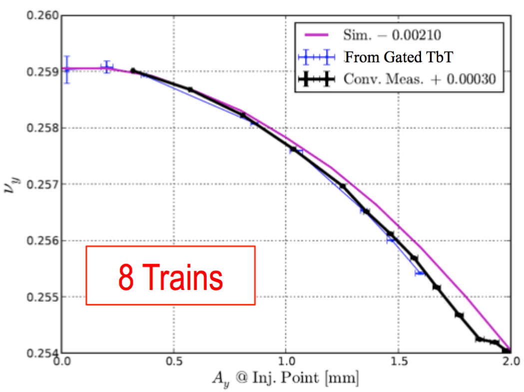

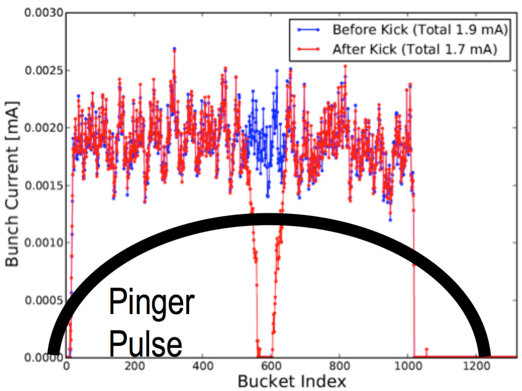

- Successful single-shot tune shift measurements obtained.
- Combination of BxB data with gated TbT amplitude data shows clear distortion around $\nu_x = 0.2$ ($5\nu_x$ resonance).
- Also single-shot dynamic aperture (DA) measurement is also possible with pinger & fill pattern monitor.

Accurate impedance measurements using gated turn-by-turn BPM data

B. Podobedov, W.X. Cheng, Y. Hidaka, IPAC'16, IBIC'16.

- At NSLS-II, transverse tunes could be measured very accurately, $<10^{-6}$, but tune stability is only $\sim 10^{-4}$.
- We figured out how to accurately measure tunes of different charge bunches stored together.
- **Example**: ping two stored bunches. From simultaneously recorded TbT positions get the tunes of each bunch.
- Tune difference is resolved to few units of 10^{-6}.

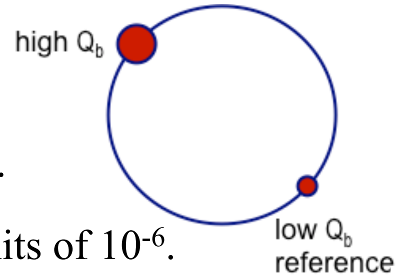

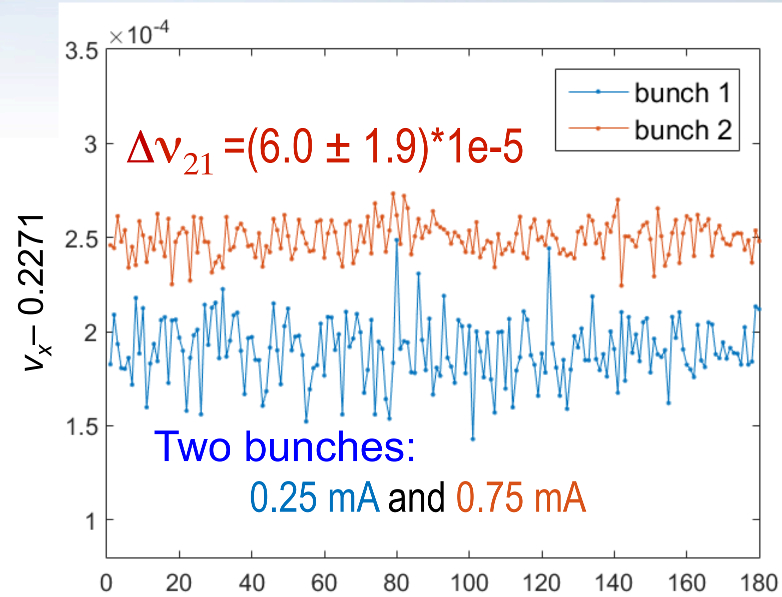

=> Very small current-dependent tune-shifts can be measured.

=> Combined with local bumps we can measure very small impedances of vacuum chamber components

$$\delta k_{kick} = 4\pi\delta(\overbrace{\nu_{lowQ_b} - \nu_{hiQ_b}}^{\text{resolve tunes to } 10^{-6}})\frac{E/e}{\Delta Q_b < \beta_x >}$$

get kick factors as low as 10 V/pC/m*

*assumed 1 nC, β =4 m, 3 GeV, σ=20 ps

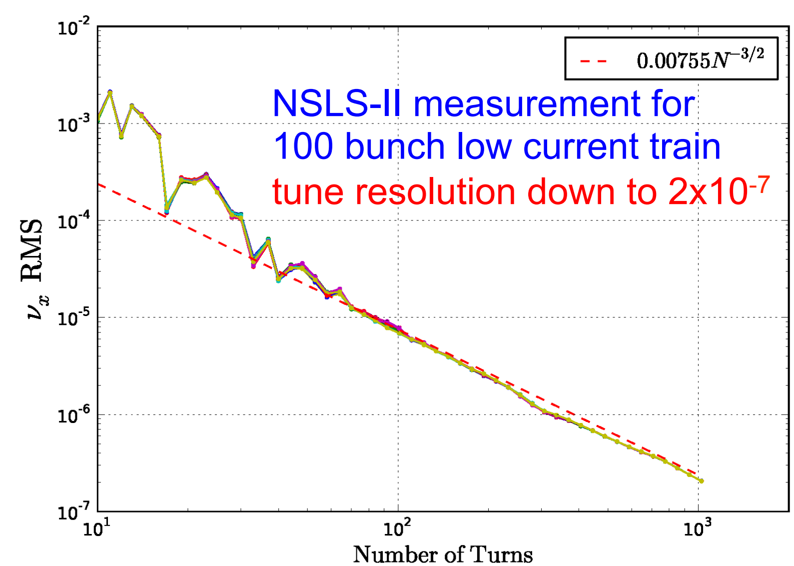

Low-frequency quadrupole impedance of undulators and wigglers

A. Blednykh, G. Bassi, Y. Hidaka, V. Smaluk, G. Stupakov, "Low-frequency quadrupole impedance of undulators and wigglers", Phys. Rev. Accel. Beams 19, 104401 (2016).

Damping wiggler chamber cross section with magnet gap closed, $d_{dw} > t_{dw} + b_{dw}$ and $t_{dw} \ll b_{dw}$.

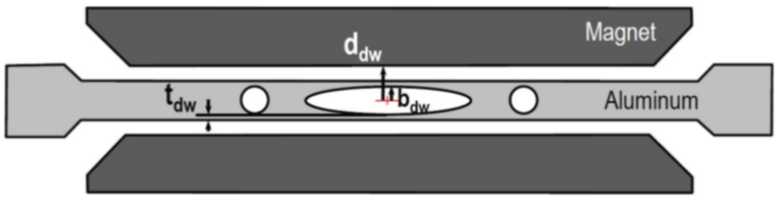

$$Z^{IVU}_{Qx,y}(d) = \pm i \frac{\pi^2}{12c(d-t)^2}\left(1 + 2\frac{(d-t)^2}{d^2}\mathrm{f}(\eta)\right)$$

$$Z^{DW}_{Qx,y}(d) = \pm i \frac{\pi^2}{12cb^2}\left(1 + \frac{2b^2}{d^2}\mathrm{f}(\eta)\right)$$

$$\Delta\nu_{x,y} = \frac{I_{av}L}{4\pi E/e}\beta_{x,y}\mathrm{Im}Z_{Qx,y}(0),$$

Damping wiggler at open position and the aluminum vacuum chamber (side-view)

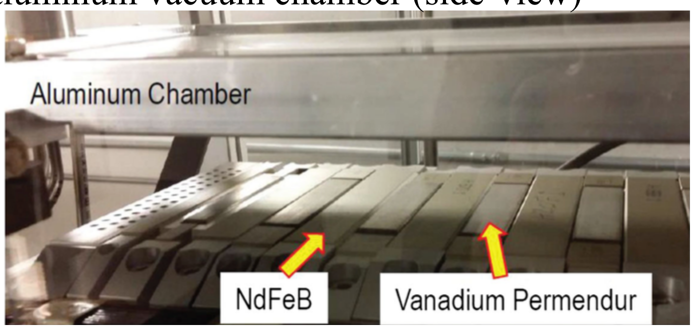

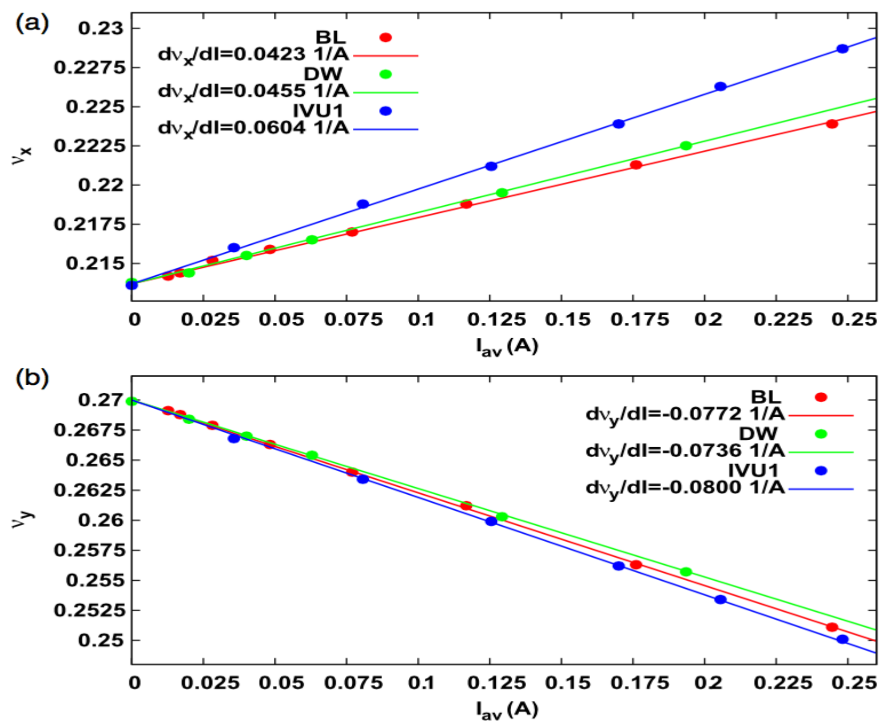

IVU without side cover

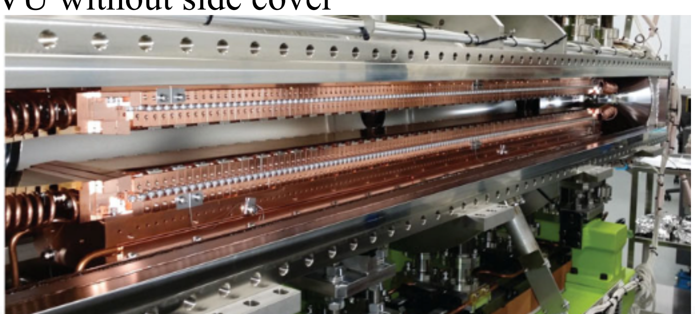

Microwave instability studies

A. Blednykh, B. Bacha, G. Bassi, Y. Chen-Wiegart, W.X. Cheng, O.V. Chubar, A.A. Derbenev, V.V. Smaluk, "Microwave instability studies in NSLS-II", NAPAC'16, Chicago, 2016 (WEA1CO05).

A. Blednykh, B. Bacha, G. Bassi, W. Cheng, K. Chen-Wiegart, O. Chubar, M. Rakitin, V. Smaluk, M. Zhernenkov, "Numerical and experimental studies of the microwave instability", NSLS-II Technical Note 239 (2017).

Synchrotron Light Monitor (SLM)

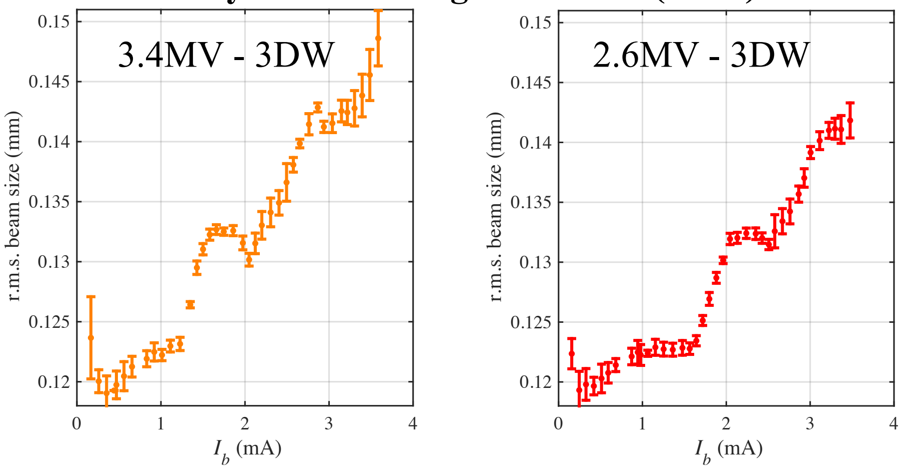

IVU vs SLM

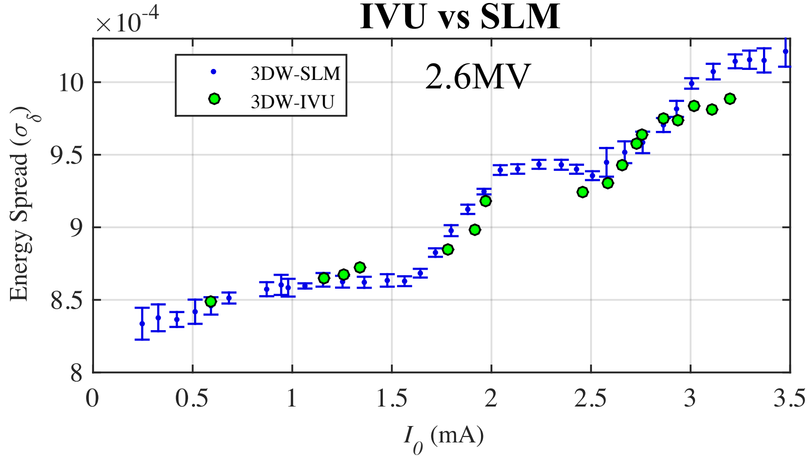

Summary of the measured single-bunch instability thresholds at different RF voltages for 3DW lattice

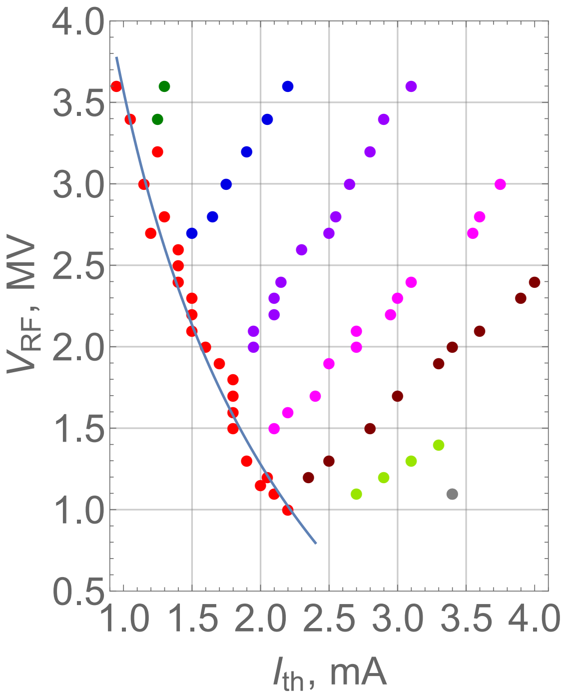

IVUs of SMI, SRX, IXS and SMI beamlines used as diagnostic tools to determine the energy spread.

Fast ion instability at NSLS-II

W. Cheng, Y. Li, B. Podobedov, "Experimental evidence of ion-induced instabilities in the NSLS-II storage ring", Accepted for publication in NIM A (2017).

- Numerous evidence of fast-Ion instability has been observed at NSLS-II.
- Instability improves with vacuum conditioning, but it is still present, esp. at low ε_y.
- Touschek lifetime increases along the bunch train => implies vertical beam size blow-up.
- Bunch-by-bunch feedback cures the centroid motion, not the beam size blow-up => could be a challenge for higher brightness light sources.

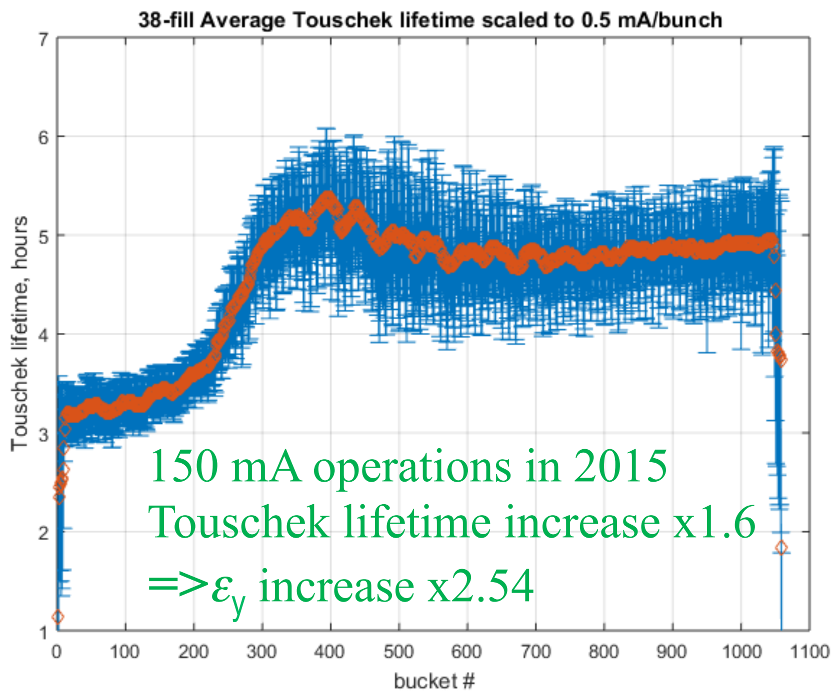

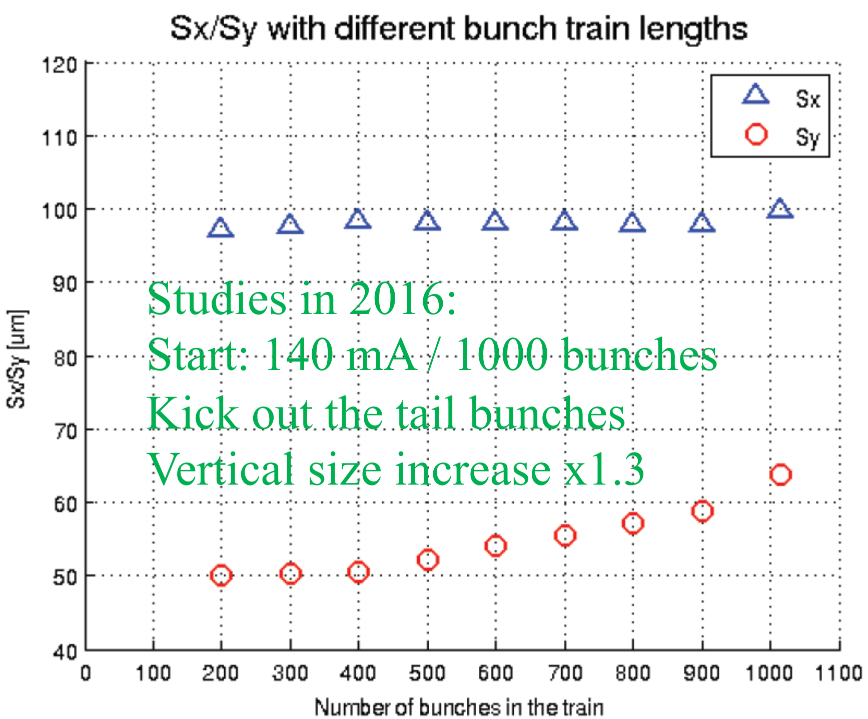

Beam dynamics with 3rd Harmonic Cavity

G. Bassi

Storage Ring Parameters

Parameter	Value
Beam energy	E = 3GeV
Average Current	I = 500mA
Number of bunches	M = 1000
Harmonic number	h = 1320
Circumference	C= 792m
Bunch length w/o HC	σ_τ= 14.5ps
Energy loss per turn	U_s=664keV
Long. radiation damping	τ_{rad}=11.9ms

SC Cavity System

2 MAIN cavities+ **3rd HARMONIC** cavity

Per cavity parameter	Value
RF frequency (main)	f_{rf} = 499.68MHz
RF frequency (3rd harmonic)	$3f_{rf}$ = 1499.04MHz
RF voltage (main)	V = 1.23MV
Beta coupling	β = 9615
Shunt impedance (main)	R_L = 33375 MΩ
Quality factor (main)	Q_L =78000
Shunt impedance (Landau)	R_H = 22880 MΩ
Quality factor (Landau)	Q_H = 2.6x10^8

Theoretical Bunch Lengthening from Active 3rd HC

bunch lengthening u for an equilibrium distribution ρ_e in quartic potential

$$u := \frac{\sigma_{\tau L}}{\sigma_{\tau m}} = \left(\frac{\Gamma(3/4)}{\Gamma(1/4)}\right)^{1/2}\left(\frac{24\cos\phi_{s0}}{(m^2-1)\omega_{rf}^2\cos\phi_s}\right)^{1/4}\frac{1}{\sqrt{\sigma_{\tau m}}} \tag{18}$$

where Γ is the Gamma function, $\sigma_{\tau_m} = \frac{\eta}{\omega_{s0}}\sigma_\delta$ is the equilibrium bunch length with only the main cavity, and σ_{τ_L} is the equilibrium bunch length with the Landau cavity. The

For the NSLS-II with σ_τ=14.5ps: $\boxed{u=3.7}$

Bunch lengthening factor u

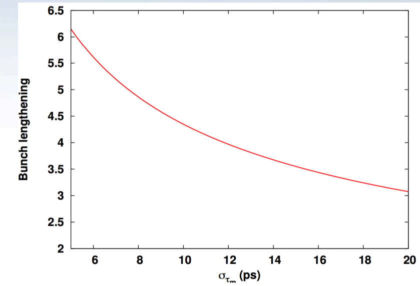

Bunch lengthening measurements: ~ 10ps/1mA

(W.Cheng, B. Bacha, Mar 4, 2016)

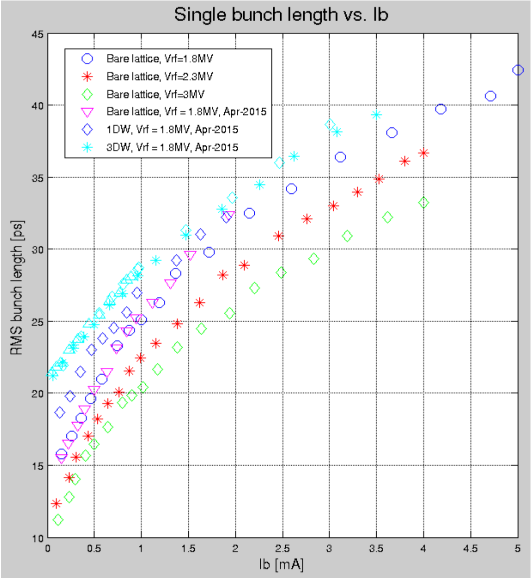

Simulations of active HC + bunch lengthening (uniform fillings)

SPACE simulations with the current longitudinal impedance budget

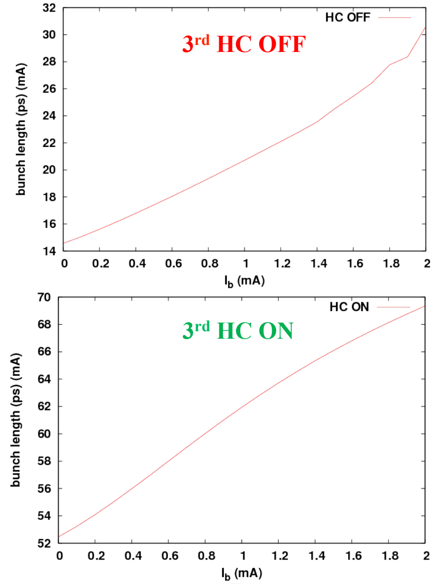

Bunch lengthening from 3rd HC weakly affected by longitudinal Impedance

Self-consistent Parallel Tracking Code SPACE

(Self-consistent Parallel Algorithm for Collective Effects)

G. Bassi, A. Blednykh and V. Smaluk, "Self-consistent simulations and analysis of the coupled-bunch instability for arbitrary multi-bunch configurations", Phys. Rev. Acc. Beams 19, 024401, (2016).

General Features and Capabilities

- Efficient study of short and long-range wakefield effects in 6D phase-space.
- Study of slow head-tail effect + coupled-bunch instabilities.
- Passive higher harmonic cavity effects with arbitrary fillings.
- Microwave instability. Efficient density estimation methods from particles.

General Parallel Structure

- M bunches each with N simulations particles distributed to M processors.
- Short-range (single bunch) wakefield interaction calculated in serial (locally).
- Long-range wakefield calculation done in parallel (globally) via master-to-slave processor communications by storing the "history" of bunch moments.
- For efficient study of microwave instability, the calculation is done in parallel by distributing N/M simulation particles to M processors.

Future Additions

- Model transverse feedback system, ion effects, LLRF.

High-brightness lattice upgrade

W. Guo, E. Blum

- Minimizing <*H*>:
  - theoretical limit: 1nm vs 2nm; theoretical minimal β_x: 0.25m vs 0.68m;
  - **Not effective**, 10-15% reduction limited by the sextupole strength.

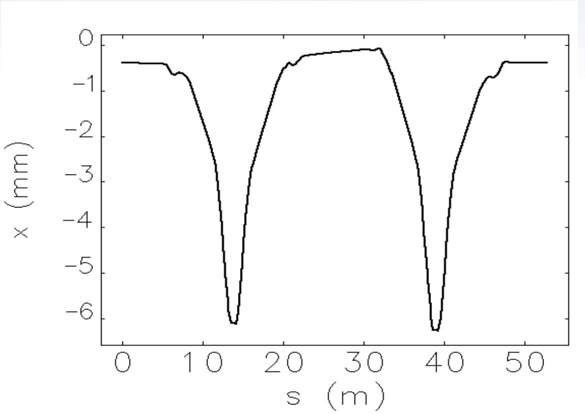

- Relaxing the achromat condition(long straights only): theoretical 0.7nm
  - 50% reduction achievable while maintaining similar lattice functions;
  - Damping wiggler sections must be dispersion-free;
  - ID provides excitation rather than damping;
  - Users of the long straights will not benefit.
- 4-bend achromat: major upgrade, challenging nonlinear optimization, emittance 0.5nm.
- **Emittance reduction by changing damping partition:**
  - ✓ Increase dipole current by about 5-10A;
  - ✓ Peak orbit change is about -6mm;
  - ✓ Rematch the quadrupoles.
  - ✓ 3-pole wiggler beamline needs to be realigned. The angular deviation is 0.7mrad (pointing outboard); however it stays within the present front end acceptance of 3.25mrad.
  - ✓ Ray tracing and top-off must be redone to ensure radiation protection.
  - ✓ Interlock values must be re-set.
  - ✓ Emittance with 3-DW is 0.6nm

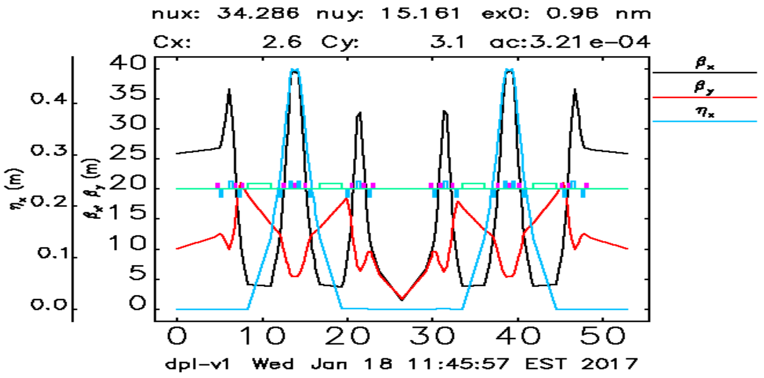

Emit	Sig d	Jx	JE
1 nm	0.06%	1.58	1.42
2 nm	0.05%	1.0	2.0

Summary

- Linear lattice correction.
- Nonlinear beam dynamics.
- Orbit correction and feedbacks.
- Beam diagnostics methods.
- Collective effects, impedances and instabilities.
- Beam dynamics with 3rd Harmonic Cavity.
- New light-generating devices.
- Injector optimization.
- High-brightness lattice upgrade.
- UED/UEM project (LDRD).
- Beam-beam interaction studies for a ring-ring based electron-ion collider (LDRD).

Thank you for your attention!